

FIELD PARAMETRISATION FOR THE ESS SUPERCONDUCTING CAVITIES

T. Lindqvist, E. Laface*
ESS, Lund, Sweden

Abstract

Here we present a method for constructing a parametrization of the electric field in the superconducting elliptic cavities of the ESS linac. The parametrization is done by replicating the electric field from measured data using trigonometric and exponential functions. The field generated by the parameters exhibits a mean error of 0.28% (maximum error of 3.8% and s.t.d. error 1.1%), with the advantage of only taking up a fraction of the required data. The field in the entire cavity is extrapolated by combining the Maxwell equations with the parametrized form of the field. We also present particle simulations based on the parametrization model to showcase some typical accelerator behaviour. Additionally we present a small extension of the parametrization method to also model spoke cavities.

INTRODUCTION

To reach the 5 MW beam power required by the ESS linac there are two non-linear components that have to be designed carefully: the space charge and the radio frequency cavities. In the high-energy section of the linac the interaction between particles and the accelerating RF-field will dominate the dynamics over the space-charge effect. The high-energy section of the linac is composed of superconducting spokes and elliptic cavities inside which a RF-field is generated and used to accelerate particles. The demand for accuracy is high since losses of particles can be harmful to the components of the accelerator.

In this paper a model for the electro-magnetic field of the RF cavities is presented. The model has been selected to allow flexibility in simulations and to reduce the amount of data required to describe the field. The field inside the RF-cavities will be parametrized, allowing the field to be described using only a small set of parameters. The RF cavities will push the particles in the beam with a peak surface field of 30 MV/m. This acceleration influences the longitudinal dynamics of the beam producing a strong non-linear behaviour with respect to the longitudinal position of particles in the beam. In order to model the acceptance of the linac the dynamics of each particle is modelled by using a field map to describe the field inside each cavity. Acceptance is defined as the set of the accepted particle, and a particle is defined as accepted if it remains in the vicinity of the synchronous particle at the end of the beamline. This model omits to include space-charge forces and the only transversal force is generated by the the RF-cavities itself.

CAVITY MODEL

The model for the ESS simulations used here is the ESS Linac Simulator (ELS). It implements a so-called kick-drift-kick model for the cavity where the force is integrated and applied as an instantaneous thin kick using matrices [1]. Such a model requires the calculation of the transit time factor in advance for the reference particle. Also the phase and the energy has to be pre-calculated in the spoke and elliptical cavities, based on the distance between the gaps. The thin kick approximation was proved to be in good agreement with the proper field integrator presented in the TraceWin code [2], for particles close to the synchronous particle [1]. However, when the energy of a particle differs significantly from that of the synchronous particle the energy gain and phase advances are systematically wrong. To avoid this problem, a new cavity model was developed which using a small number of parameters that regenerates the original field [3]. The advantage of the parametrization versus the field map is the limited number of parameters required to describe the field along the longitudinal axes. At the same time it allows the user to take into account the off-axis dynamics.

The field is divided in three main regions: the input cell, the inner cells and the output cell. The input and output cells are divided again in two sections: the inner-side sinusoidal field and the outer-side exponential decay field as shown in Fig. 1. To include the field asymmetry due to power coupler, High Order Modes (HOM) coupler or different beam tube apertures, the input and output cells are treated independently.

The inner cells (III) are modelled as the sum of first and third harmonic oscillations; the inner-side end-cells (II/IV) are modelled using the same method, but with a different wave number, while the exponential decay cells are modelled with a exponential function which takes a Gaussian form when the power of the exponent is 2. The parameters describe the field on the longitudinal axis, i.e. in the direction of the beam line.

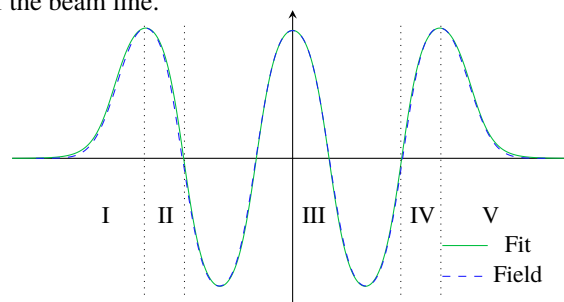


Figure 1: The numerical field vs. the fit with the trigonometric model. The input/output exponential decay (I/V), input/output sinusoidal (II/IV), and inner cells (III).

* Emanuele.Laface@esss.se

The matching against the field map data for the sinusoidal cells is done using the least square method, and the matching parameters for the exponential decay cells are calculated analytically. To recreate the field, 15 parameters are required: geometric β of the cavity (β_g); number of cells; frequency (f_{rf}); amplitude of the first and third harmonic for the inner cells, input cells, and output cells; the gap shift for the input and output cells; and exponent power and σ of the input and output cells. In order to use this field in the simulations the synchronous phase needs to be included. On the other hand the synchronous phase is not needed to describe the field and is therefore not considered here.

The field in the regions I and V is:

$$F(z) = A_{\exp} \cdot e^{-\left(\frac{|z-L_{\exp}|}{2\sigma_{\exp}}\right)^{p_{\exp}}}, \quad (1)$$

where A_{\exp} is the coefficient of the exponential; L_{\exp} is the position of transition from region I to II (IV to V) for the input (output) cells; σ_{\exp} represents the width of the decay field; p_{\exp} is the power of the exponential. Both σ and p could be found analytically by using the data from a measured field. The parameters A_{\exp} and L_{\exp} are derived from the parameters in section II and IV.

The equation describing the field in the regions II and IV is:

$$F(z) = B_1 \cdot \cos\left(2\pi \frac{z - \phi_1}{L'}\right) + B_3 \cdot \cos\left(6\pi \frac{z - \phi_3}{L'}\right), \quad (2)$$

where B_1 and B_3 are the coefficients for the first and third harmonic, ϕ_1 and ϕ_3 are phases to make the function continuous at the transition between region II and III (III and IV) for the input (output) cells, and L' is the adjusted cell length. The parameters L' , B_1 and B_3 are calculated from measured field data while the phases ϕ_1 and ϕ_3 are derived from the parameters of section III.

The field in the inner cells is generated using:

$$F(z) = A_1 \cdot \cos\left(2\pi \frac{z}{L}\right) + A_3 \cdot \cos\left(2\pi \frac{3z}{L}\right),$$

where A_1 and A_3 are the coefficients of the first and third harmonic for the inner cells, and L is the period length equal to $\beta_g \lambda$ ($\lambda = c/f_{rf}$). They are all calculated from measured field data.

To evaluate the goodness of the model, the Transit Time Factor (TTF) is calculated with the trigonometric fit and compared with the field map. The result is shown in Fig. 2.

The field can be extended to model off-axis particle dynamics by solving the wave equation in a cylindrical geometry:

$$\left(\nabla - \frac{1}{c^2} \frac{\partial}{\partial t}\right) R(r) \cos\left(\frac{\pi m z}{L}\right) \sin(\omega t) = 0. \quad (3)$$

This equation assumes that the field has an entirely cosinusoidal shape along the z -axis, which is not completely true, but it is a fair approximation for particles close to the z -axis. The field in the cavities is assumed to be excited in

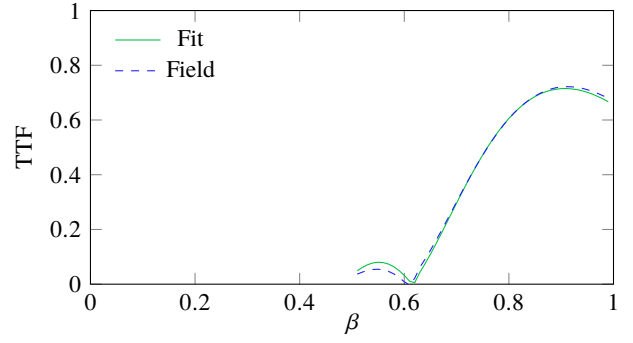


Figure 2: TTF calculated for a range of synchronous β using the field from RF simulations and the fitted field.

the TM_{010} -mode. The three components of the field that influence particle dynamics are [4]:

$$E_z(r, z, t) = \sum_{m=1,3} A_m J_0(k_m r) \cos\left(\frac{\pi m z}{L}\right) \sin(\omega t) \quad (4)$$

$$E_r(z, r, t) = - \sum_{m=1,3} \frac{A_m}{k_m} J_1(k_m r) \frac{\partial \cos(\pi m z/L)}{\partial z} \sin(\omega t) \quad (5)$$

$$B_\theta(z, r, t) = \sum_{m=1,3} \frac{A_m \omega}{k_m c^2} J_1(k_m r) \cos\left(\frac{\pi m z}{L}\right) \cos(\omega t). \quad (6)$$

Where J_0 and J_1 are Bessel functions of zeroth and first order, L is defined in the parametrization and gives the longitudinal scaling of the function, m is the order of the harmonic, ω is the angular frequency of the field, and r is the radial coordinate. The constant k_m gives the radial scaling of the Bessel functions, and is found by ensuring that the wave equation (3) is fulfilled, by solving

$$k_m^2 = \left(\frac{m\pi}{L}\right)^2 + \left(\frac{\omega}{c}\right)^2. \quad (7)$$

The radial structure of the field, presented above is maintained in the outer sections (I/IV), but in these sections it does not couple to the analytical expression of the parametrization via the wave equation. An examination of the frequency content of the complete longitudinal field in one cavity yields the Table 1:

Table 1: Frequency Content Normalized Around First Harmonic

Harmonic	Amplitude
1st	1
3rd	$-5.21 \cdot 10^{-2}$
5th	$3.84 \cdot 10^{-3}$
7th	$-2.79 \cdot 10^{-4}$
9th	$2.29 \cdot 10^{-5}$

The Fourier analysis shows that the power contained in the higher order harmonics decreases by an order of magnitude for every step up in harmonic. The radial solution is good even in the outer sections of the cavity. A reconstruction of the field can be seen in Fig. 3. The difference between the field reconstructed from the parametrization compared to the measured data is on average 0.28% with a standard

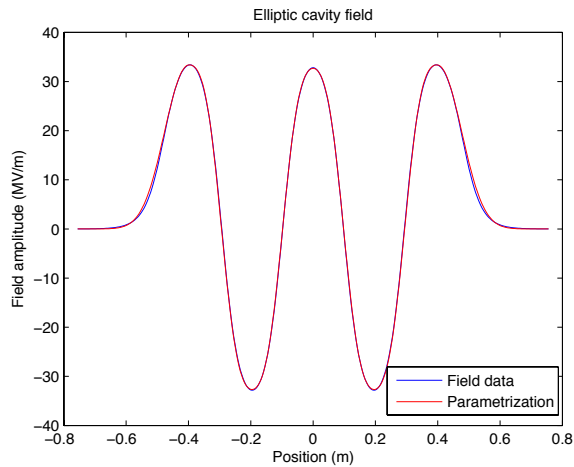


Figure 3: The parametrization overlapping the field data.

deviation of 1.1%. The parametrization presented here has been extended to the spoke cavities by adding the 5:th harmonic to the cosine expansion of the field. This requires the use of three additional parameters, where the parameters are the amplitude of the fifth harmonic in the sections from II to IV. The result can be seen in Fig. 4, where the mean difference is 0.22%, and the standard deviation is slightly larger, 1.6%, again with respect to the maximum amplitude of the measured data.

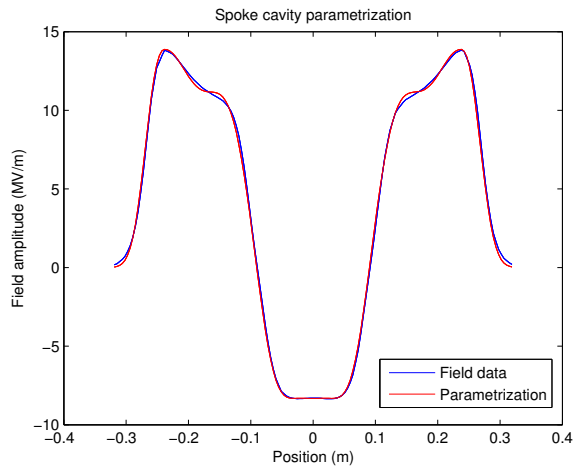


Figure 4: The field obtained through the parametrization together with a measured field inside a spoke cavity.

PARTICLE SIMULATIONS

The high- β section of the ESS linac is simulated using the trigonometric model integrating the field with a simple second order scheme. It replicates the energy gain for the synchronous particle within 99.9% of the expected value. It also predicts the behaviour of particles far from the synchronous particle. Figure 5 shows the density plot of the accepted particles simulated from a gaussian distribution at the entrance of the high- β section. It exhibits the expected 'golf-club' shape [5].

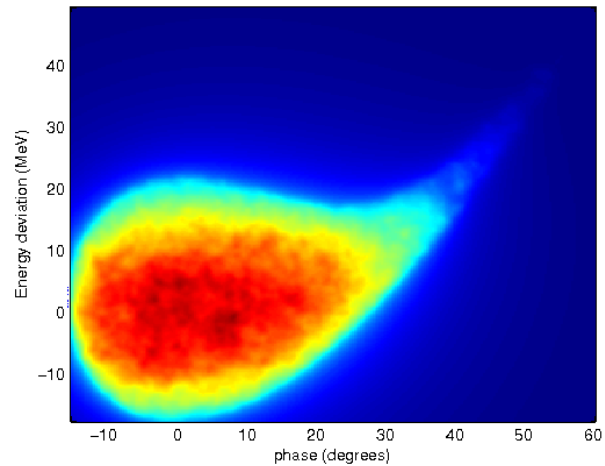


Figure 5: Accepted particles at the entrance of the ESS high- β section.

Further Development

The model can be developed further by improving the particle integration algorithm beyond a simple second order Runge-Kutta scheme. Another step towards making the results more realistic is by adding a method that accounts for particle-particle interaction, such as presented in [4].

CONCLUSION

The proposed RF model is able to generate the field map for multi-gap cavities based on 15 parameters. It exhibits an average error with respect to the classic field map, of 1.1% for elliptical cavities and 1.6% for spoke cavities. The model can be used, together with a particle simulator, to examine various configurations of the linac and predict its performances and behaviour. As a test case the synchronous particle is simulated in the high- β section of the ESS linac and the model predicts its energy gain within 99.9%. The model also successfully produces expected configurations in phase space for particle bunches. The model can be used, for example, to evaluate the problem of optimization presented in [6].

REFERENCES

- [1] E. Laface *et al.*, "The ESS Linac Simulator: a first benchmark with TraceWin," *Proc. of IPAC 2013, Shanghai, China*, May 2013.
- [2] D. Uriot. TraceWin: <http://irfu.cea.fr/Sacm/logiciels/index3.php>
- [3] T. Lindqvist, "Field parameterization by trigonometric expansion combined with particle tracking in superconducting cavities", Master's thesis, Lund University, November 2013.
- [4] E. Laface *et al.*, "Space Charge and Cavity Modeling for the ESS Linac Simulator," *Proc. of IPAC 2013, Shanghai, China*, May 2013.
- [5] T. P. Wangler, *RF Linear Accelerators, 2nd. Completely Revised and Enlarged Edition*, ser. Physics textbook. Weinheim: Wiley-VCH, Jan. 2008.
- [6] S. Peggs *et al.*, "Sorting in the ESS", *Proc. of IPAC 2014, Dresden, Germany*, June 2014.